Geol. Mag. **149** (*5*), *2012, pp. 819–826. © Cambridge University Press 2012*
doi:10.1017/S0016756811001075

Simple shear is not so simple! Kinematics and shear senses in Newtonian viscous simple shear zones

SOUMYAJIT MUKHERJEE*

Department of Earth Sciences, Indian Institute of Technology Bombay, Powai, Mumbai-400 076, Maharashtra, India

(*Received* 28 June 2011; *accepted* 18 November 2011; *first published online* 17 January 2012)

Abstract – This work develops an analytical model of shear senses within an inclined ductile simple shear zone with parallel rigid boundaries and incompressible Newtonian viscous rheology. Taking account of gravity that tends to drive the material downdip and a possible pressure gradient that drives it upward along the shear zone, it is shown that (i) contradictory shear senses develop within two sub-zones even as a result of a single simple shear deformation; (ii) the highest velocity and least shear strain develop along the contact between the two sub-zones of reverse shear; (iii) for a uniform shear sense of the boundaries, a zone of reverse shear may develop within the top of the shear zone if the pressure gradient dominates the gravity component; otherwise it forms near the bottom boundary; (iv-a) a 'pivot' defined by the intersection between the velocity profile and the initial marker position distinguishes two sub-zones of opposite movement directions (*not* shear sense); (iv-b) a pivot inside any non-horizontal shear zone indicates a part of the zone that extrudes while the other subducts simultaneously; (v) the same shear sense develops: (v-a) when under a uniform shear of the boundaries, the shear zone remains horizontal and the pressure gradient vanishes; or alternatively (v-b) if the shear zone is inclined but the gravity component counterbalances the pressure gradient. Zones with shear sense reversal need to be reinterpreted since a pro-sheared sub-zone can retro-shear if the flow parameters change their magnitudes even though the same shear sense along the boundaries is maintained.

Keywords: simple shear, shear zone, shear sense, Poiseuille flow, viscosity, extrusion, Newtonian fluid.

1. Introduction

Simple shear in ductile shear zones is a deformation where the boundaries of the zone move parallel to themselves relative to each other (e.g. Twiss & Moores, 2007, pp. 330–1). Since geological deformations take place at exceedingly slow rates, usually ranging from a fraction of a millimetre per year (e.g. Wobus, Heimsath & Whipple, 2005 and references therein) up to a few centimetres per year (as referred to in Annen, Scaillet & Sparks, 2005), simple shearing of plastically deforming rocks inevitably leads to creep. Thus, simple shear in geology leads to very slow laminar motion of material points, with a Reynolds Number of the order of $\leq 10^{-15}$ (Mukherjee & Koyi, 2010*a,b*).

Ductile deformation of rocks is conventionally modelled by flowing fluids (Ramsay & Lisle, 2000). Here simple shear is equated with Couette flow (in the sense of Schlichting & Gersten, 1999) and Poiseuille flow to describe fluid flow through static infinitely long parallel boundaries (Pai, 1956). The boundaries of Poiseuille flow could have any spatial orientation, cross-section geometry and dip (in the sense used by Pai, 1956; Schlichting & Gersten, 1999).

Better understanding of ductile shear zones, and hence their shear sense, is of fundamental importance in plate tectonics since such zones define plate boundaries (including collisional mountains) (Regenauer-Lieb & Yuen, 2003). In the last 30 years or so, previous workers (such as England & Holland, 1979; Moores & Twiss, 1995) envisaged simple shear as one of the possible mechanisms of subduction and underplating of sediments through inclined zones with parallel boundaries. For example, in his figure 6.39, Stüwe (2007) described parabolic patterns in a subduction zone of parabolic profiles. The component of flow that tends to extrude rocks along the channel was mentioned as 'hydraulic potential', and any shear that tends to produce a linear profile if the zone is horizontal as 'drag'. Another reason why understanding the theory of ductile shearing through field studies and/or modelling is crucial is that shear can also modify pre-existing ore deposits (e.g. Evans, 1980).

This work investigates the kinematics of simple shear and the development of shear senses in ductile simple shear zones and their significance in extrusion. Shear fabrics (see Passchier & Trouw, 2005 for review; Mukherjee, 2011) allow deducing only the relative sense of movement of the shear zone boundaries. Notwithstanding, this study considers absolute movement of the boundaries. The way folds and microstructures evolve are not addressed.

2. The model

A kilometre-scale shear zone with parallel, dipping, very long and rigid boundaries is here considered to have the rheology of an incompressible Newtonian viscous fluid, in which applied stress and the resultant

*E-mail: soumyajitm@gmail.com

strain rate are proportional (Schlichting & Gersten, 1999). The bottom end of the shear zone is assumed to have a pressure higher than the top end. This gives rise to a pressure gradient that tends to drive rock up the shear zone. The boundaries of the shear zone are considered to undergo reverse-sense simple shear (Figs 1–3). The 'Poisson equation' of flow (Eqn 1 in the Appendix) is chosen to deduce the velocity profile. This flow equation is equated with deformation in ductile shear zones as it has been adopted by previous workers (e.g. Grujic *et al*. 1996; Ramsay & Lisle, 2000; Grujic, Hollister & Parrish, 2002; Stüwe, 2007; Mancktelow, 2008). The co-ordinate axes are chosen such that the positive direction of the *z*-axis is in the updip direction (Figs 1–3). A component of gravity, given by the product of density, acceleration due to gravity and the sine of the dip of the shear zone, tends to drive the rock downward between its parallel dipping boundaries (Eqns 1 and 2 in the Appendix). The gravity component counteracts the pressure gradient and tends to extrude the rock.

The presence of these components can be understood from field studies and mechanical considerations. For example, (i) the relative movement of the shear zone boundaries is exemplified by a number of shear sense indicators, most ubiquitously by S–C fabrics and mineral fish (Berthé, Choukroune & Jegouzo, 1979; Passchier & Trouw, 2005; Mukherjee, 2011). (ii) The presence of leucosomes in sheared migmatites, boudins, pressure shadows and solutions, veins and reaction textures indicate the activity of a pressure gradient along the shear zone (Mancktelow, 2008; also Hollister, 1993; Li, Gerya & Burg, 2010). Schulmann *et al*. (2008) categorized tectonic models of extrusion (of the ultrahigh pressure rocks) into (a) corner flow in an accretionary wedge with buoyancy-driven extrusion; (b) gravity-driven exhumation guided either by removal of the mountain roots; and (c) focused erosion or topographic load driven the flow of partially molten rocks along sub-horizontal channels driven by either focused erosion or topographic load. Apart from these, a fourth method involving (b) and (c), i.e. buoyancy-driven extrusion augmented by erosion, has also recently been modelled by many (e.g. Weinberger *et al*. 2006; Warren, Beaumont & Jamieson, 2008*a–c*; Whipple, 2009). In all these cases, pressure gradient is implicit in fluid mechanical derivations. Deviatoric stress that leads to ductile deformation of rocks in tectonic contexts (Li, Gerya & Burg, 2010) can also create a pressure gradient, which could ultimately be correlated with lithostatic pressure gradient (Grujic *et al*. 1996; Vannay & Grasemann, 2001; Godin *et al*. 2006). Alternately, even a small percentage of melt would favour buoyant extrusion along the shear zone and develop a pressure gradient (Beaumont *et al*. 2001). (iii) In tectonic scenarios, an inclined shear zone will always have its component of weight acting in the downdip direction.

Under these conditions, the velocity profile within the shear zone is usually a parabola, and *not* a straight line. A line passing through the vertex of the profile that parallels the shear zone boundaries divides the whole zone into two unequal sub-zones of opposite ductile shear senses (Fig. 1b–f). As in a purely Poiseuille flow, the vertex is also the point of fastest velocity and least shear strain in the shear zone. The velocity profile depends on the following parameters: (i) the absolute velocities of the two boundaries; (ii) thickness and (iii) dip of the shear zone; (iv) acceleration due to gravity; (v) pressure gradient along the shear zone; and (vi) density and (vii) viscosity of the rock (Eqn 3 in the Appendix). Several specific cases and the corresponding velocity profiles are presented as follows.

I. A case in which the sense of shear throughout the zone is identical, and, independent of density and acceleration due to gravity, is for any dip of the shear zone where the effect of gravity and the pressure gradient nullify each other (the case of Eqn 11 in the Appendix). This is the case that matches the homogeneous simple shear of a pack of cards depicted in many textbooks.

II. When the boundaries are sheared and the pressure gradient overpowers the component of gravity, the convex side of the parabolic profile points updip along the shear zone (Fig. 1b, e). While the sub-zone in contact with the lower boundary acquires the same shear sense as that of the shear on the boundaries, the smaller sub-zone at the top undergoes a reverse shear. In other words, while a narrower zone of ductile normal shearing forms in contact with the upper boundary, a wider zone of reverse shear develops in contact with the lower boundary.

III. When the component of gravity exceeds the pressure gradient, and the boundaries are sheared, the parabolic profile is convex downdip. The vertex of the flow profile in this case is closer to the lower boundary of the shear zone (Fig. 1c, d, f). In this case, while a narrower sub-zone in contact with the lower boundary develops a normal shear sense, opposite to the reverse shear sense between the two boundaries, the other wider sub-zone at the top acts as a ductile thrust with the same shear as that on the boundaries.

In the two latter cases (II and III), the imaginary lines that parallel the shear zone boundaries and pass through the vertices demarcate a thinner sub-zone in which the shear sense reverses. Under certain algebraic relations among the seven flow parameters, the vertices of the parabolic velocity profiles touch one of the boundaries (curve A in Fig. 2a and 2b for cases II and III, respectively), or can even plot outside the shear zone (curve B in Fig. 2a and 2b for cases II and III, respectively). In such situations, a uniform shear sense develops across the complete width of the shear zone.

IV. The point at which the velocity profile (or its extrapolation outside the shear zone) intersects the co-ordinate axis that is perpendicular to the linear boundaries of the zone (i.e. the '*y*-axis' in the figures), is denoted as a 'pivot' (Fig. 1a–e). The shear sense does not alter across the pivot as it does across the vertex. The pivot lies inside the shear zone only if the

https://doi.org/10.1017/S0016756811001075 Published online by Cambridge University Press

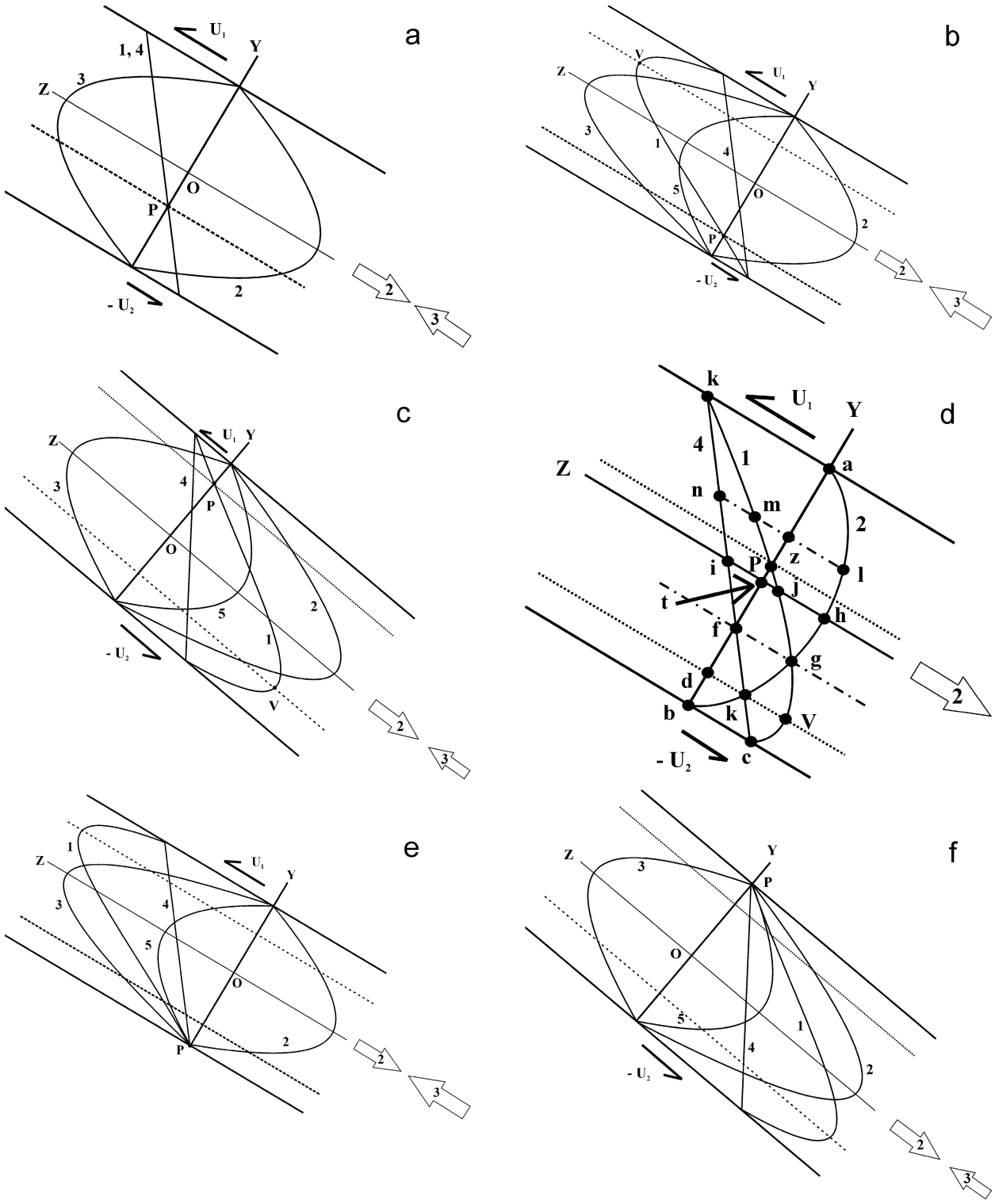

Figure 1. Simple shear of a shear zone of incompressible Newtonian fluid with parallel boundaries. The profile '3' represents the flow due to pressure gradient, '2' indicates the flow due to gravity and '1' is the resultant flow profile. The full arrows '2' and '3' represent intensities of the respective flows (similar to fig. 11 of Zhao *et al*. 2011). Profiles '4' and '5' represent the profile due to shear of the boundaries, and the resultant of profiles '2' and '3', respectively. V – vertex; P – pivot. Dashed lines passing through them mark sub-zones of opposite shear senses and sub-zones of opposite bulk movements (extrusion and subduction), respectively. (a) An inclined shear zone where the component of gravity equals the pressure gradient. The resultant is a linear velocity profile arising from shear of the boundaries. (b) An inclined shear zone where the component of gravity is lower than the pressure gradient. The resultant of these two flows has its vertex pointing updip. (c) An inclined shear zone where the component of gravity exceeds the pressure gradient. The resultant parabola has its vertex pointing downdip. (d) Combination of shear of the boundaries and the flow component of gravity in an inclined shear zone with no pressure gradient. The resultant profile '1' is deduced point by point using vector addition as follows: (nz – zl) = mz; 2 * dk = dv; (th – ti) = tj. (e) The situation is as in (b) except that $U_2 = 0$. The entire shear zone extrudes. (f) The situation is as in (c) except that $U_1 = 0$. The entire shear zone subducts.

https://doi.org/10.1017/S0016756811001075 Published online by Cambridge University Press

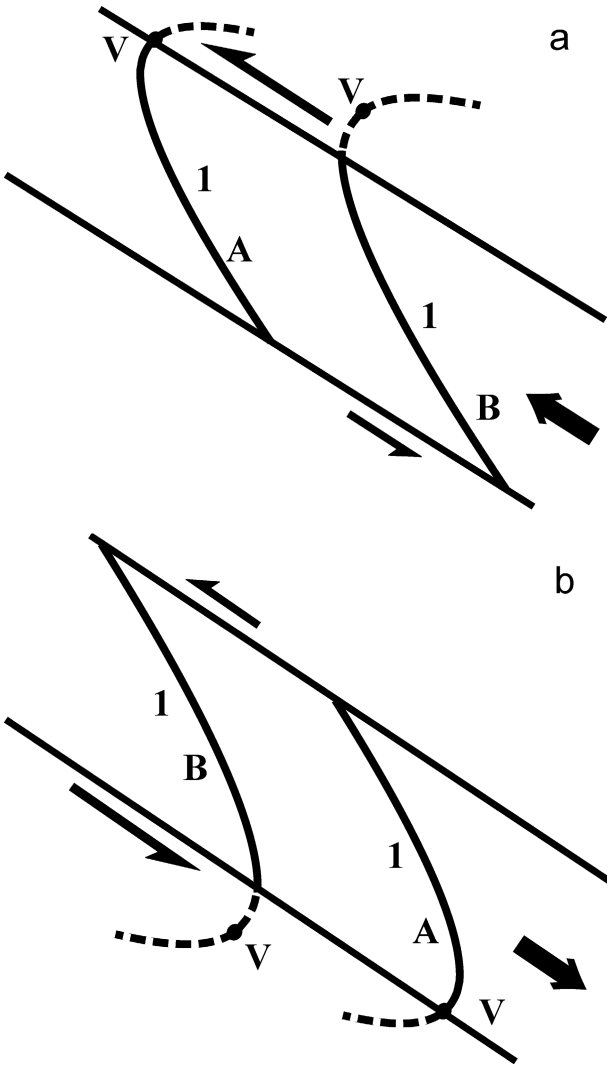

Figure 2. Two special cases of resultant velocity profiles in an inclined shear zone. In profile 'A', the vertex ('V') is coincident with the upper boundary of the shear zone, whereas in the profile 'B', it lies outside the shear zone.

two boundaries shear in opposite directions (i.e. one downdip and the other updip). In such a case, while a part of the non-horizontal (inclined or even vertical) shear zone extrudes across the pivot, the remainder subducts simultaneously. A line that parallels the shear zone boundary and passes through the pivot demarcates those two sub-zones. Along this line, all points remain static throughout the shearing process. On the other hand, (i) if both the boundaries move in the same direction (either updip or downdip), the pivot locates outside the shear zone (Fig. 3); (ii) if either of the boundaries remains stationary but the other moves, the pivot locates on the stationary boundary (Fig. 1e, f). In the last two cases, the shear zones either entirely extrude or subduct. In the cases of a dipping shear zone where the effect of gravity nullifies the pressure gradient (Fig. 1a), the position of the pivot is the same and is defined only by: (i) the thickness of the shear zone; and (ii) the absolute velocities of the shear zone boundaries (Eqn 11 in the Appendix).

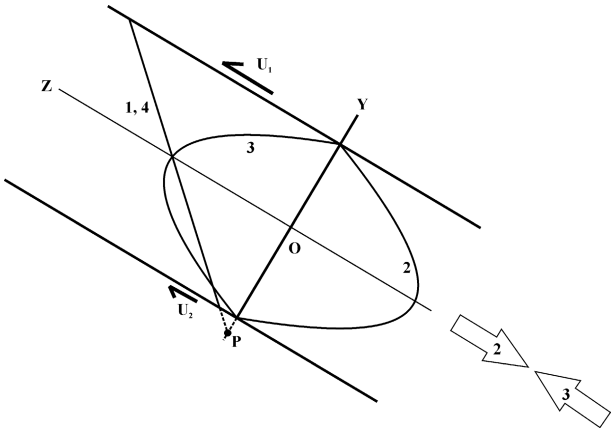

Figure 3. In an inclined shear zone, both boundaries' shear move updip, but the upper boundary moves with a greater velocity. See caption of Figure 1 for explanation of numbers for different profiles and those within the full arrows. The pressure gradient and the component of gravity are equal. Extrapolation of the resultant velocity profile meets the *y*-axis at 'P' that defines the pivot.

V. In addition to fluid mechanical derivations, various combinations of flow mechanisms can also be understood graphically. After drawing velocity profiles for different types of simple shear, vector addition of velocities is necessary to construct the resultant velocity profile (Fig. 1d and its caption). This is in conformity with fluid mechanical deductions (Eqn 15 in the Appendix).

VI. The kinematics of simple shear zones that are not a part of any large hot orogen and are devoid of the pressure gradient along them can also be worked out from the presented model by putting $\partial P/\partial x = 0$ in Eqn 1 in the Appendix. For reverse ductile shearing of the boundaries, a thicker sub-zone of reverse shear develops within the top zone and a thinner sub-zone of normal shear sense develops within the bottom boundary (Fig. 1d). As in the case in Figure 2b, if the vertex plots on the bottom boundary or even outside the shear zone, a single shear sense will develop.

3. Discussion

Any slip at the boundaries and the pressure gradient are considered two independent parameters although they could act simultaneously. An example of this is the ascent of partially molten rocks within the upper portion of the Higher Himalayan Shear Zone along with coeval ductile shear of its boundaries (reviews by Godin *et al*. 2006; Yin, 2006). The present model is set in the way that shear along the boundaries is deciphered from geochronology (e.g. Harrison *et al*. 1997; Catlos, *et al*. 2001), and the pressure gradient from geothermobarometry (e.g. E. J. Catlos, unpub. Ph.D. thesis, Univ. California, 2000) of natural shear zones could be used to predict sub-zones of reverse shear. Since the fluid mechanics (Eqn 1 in the Appendix) on which this paper is based considers

https://doi.org/10.1017/S0016756811001075 Published online by Cambridge University Press

infinitely long shear zones, it should not be applied to any metre-scale or smaller 'sporadic' shear zones.

Shear zones of conflicting (or 'opposite') shear senses have commonly been attributed to a retro-shear of the whole zone, e.g. from an initial top-to-SW into a late top-to-NE in the South Tibetan Detachment System in the Himalaya (Patel *et al*. 1993; Jain & Patel, 1999; review by Godin *et al*. 2006; Yin, 2006). Such thinking also led to postulation of specific extrusion models for the major shear zones. The present model indicates that two shear senses can form simultaneously well within any shear zone subject to a uniform simple shear of its boundaries (Fig. 1b–f).

Secondly, merely changing the magnitudes of a few of the flow parameters (shear rate, dip of the boundaries, density and viscosity of the rock types and the pressure gradient) over time can invert an early pro-shear into a late retro-shear. One such possibility could be where an initially uniform shear persisted and the pressure gradient was balanced by the component of gravity (Fig. 1a). Later the density of the rock, dip of the shear zone and the pressure gradient might change to the extent that the component of gravity becomes weaker than the pressure gradient. This would then produce an opposed shear sense near the upper boundary of the shear zone (Fig. 1b). (i) The pressure gradient along an orogen-parallel shear zone can vary by about an order of magnitude in different locations (E. J. Catlos, unpub. Ph.D. thesis, Univ. California, 2000; Fraser, Worley & Sandiford, 2000; Hollister & Grujic, 2006). The extrusion rate of an intra-continental shear zone can change significantly with time (Ganguli *et al*. 2000). (ii) The rate of slip of a shear zone boundary can vary in both space and time (Harrison *et al*. 1997; Valdiya, 2001; Catlos *et al*. 2001). (iii) The viscosity of the partially molten mid-crustal rocks could vary by 14 orders of magnitude (Scaillet, Holtz & Pichavant, 1996; Beaumont *et al*. 2001). (iv) In compressional regimes, shear zones may rotate and change their dip (Leech *et al*. 2005).

The present analytical models of simple shear investigate a reverse shear (top-to-updip). The starting equation of fluid mechanics (Eqn 1 in Appendix) also has potential for constraining shear senses for a normal shear sense (top-to-downdip) by reversing shear senses at the shear zone boundaries. Assuming similar vector addition (as in Fig. 1d) allows deduction of different flow profiles, co-ordinates of pivots and vertices, and anticipation of the development of two opposed shear senses in the general case, and in the special cases of a uniform sense (similar to Fig. 1a). In general, normal sense shear will also lead to subduction simultaneous with extrusion (similar to Fig. 1a–d).

The models presented here should be compared with natural shear zones with utmost caution because of the following possibilities. Shear zones may develop non-Newtonian behaviour (as interpreted from Dasgupta, Chakraborty & Neogi's, 2009 findings by Mukherjee & Koyi, 2010*a*) or involve molten rocks (Webb & Dingwell, 1990). The boundaries of the shear zone act rigidly only if the ratio of viscosity between the shear zone and its surroundings is $\leq 10^{-7}$ (Mancktelow, 2008). Melting during ductile shearing (Marchildon & Brown, 2003) means that the shear zone is no longer incompressible. Fluid channelling during ductile shearing can lead to up to 60 % volume loss from the middle of the shear zone (Selverstone, Morteani & Staude, 1991). Thickness of orogenic shear zones can vary by an order of magnitude (Lombardo, Pertusati & Borghi, 1993; Jain & Anand, 1988). In natural shear zones, a component of pure shear might apply either uniformly (Vannay & Grasemann, 2001), or non-uniformly (Exner, Grasemann & Mancktelow, 2006). Natural shear zones can contain more than one lithology. Assigning single values for the density and viscosity while modelling may obscure some of their kinematic details. The kinematics for a 'single lithology' may also be non-uniform because of local variations in composition or grain size.

In their advanced thermal mechanical model of extrusion induced by ductile shear, the Dalhousie group of modellers (e.g. Beaumont *et al*. 2004; also Kellett *et al*. 2010 as the latest example) considered a number of additional parameters such as geothermal gradient, radioactive heat production, thermal expansion coefficients and power law behaviour, together with density changes due to phase transition during metamorphism and extrusion augmented by focused erosion. However, this work takes a minimalist approach and considers only the most significant parameters as followed by Ramsay (1980), Ramsay & Lisle (2000) and Grasemann, Edwards & Wiesmayr (2006). In addition, the following factors were also ignored: gravitational spreading or erosion of materials extruded from the top end of the shear zone; kinematic dilatancy (Grasemann, Edwards & Wiesmayr, 2006); strain partitioning (Mancktelow, 2006); and changes in rock rheologies (von Huene, Ranero, & Scholl, 2009).

4. Conclusions

The shear senses of inclined simple shear zones with parallel long boundaries are investigated by considering them as having incompressible Newtonian viscous rheologies. A parabolic velocity profile develops with a vertex that moves fastest, denotes the point of least shear strain and lies on a line that demarcates two sub-zones of opposite shear senses. The flow profile is dependent on the size and the orientation of the shear zones, pressure gradient, density and viscosity of the rocks, and gravity. A pressure gradient stronger than the gravity component makes the parabolic profile convex upward, and a weaker one downdip. Reverse shear on this profile leads to a thinner sub-zone of normal shear developing near the top of the shear zone. The intersection between the velocity profile and a line perpendicular to the flow direction/shear zone defines the 'pivot' that remains static throughout the deformation history as long as the flow parameters remain unchanged. The pivot falls inside the shear zone if the boundaries shear in opposite directions;

https://doi.org/10.1017/S0016756811001075 Published online by Cambridge University Press

otherwise it falls outside. For an internal pivot, a part of a non-horizontal shear zone across the pivot extrudes while the other part subducts. The whole shear zone either extrudes or subducts (i) if only a single boundary of the shear zone moves and when the pivot falls on the stationary boundary; and (ii) if both the boundaries move in the same direction and the pivot falls outside the shear zone. Changes in magnitude of flow parameters can develop a sub-zone of retro-shear in contact with one of the boundaries of the shear zone where initially a pro-shear was persistent.

Acknowledgements. Supported by IIT Bombay's Seed Grant: *Spons/GS/SM-1/2009*; and Department of Science and Technology's (New Delhi) SERC Fast Track Scheme: *SR/FTP/ES-117/2009*. Chris Talbot made three rounds of in depth informal review that significantly improved the scientific content and the English. A very detailed review by Haakon Fossen, and those by Paul Bons and an anonymous reviewer of a previous version greatly improved and significantly shortened the manuscript. Interaction with Kirti Chandra Sahu helped to clarify several points. Katarzyna Piper is thanked for her thorough copyediting and Sally Thomas for technical editing.

References

ANNEN, C., SCAILLET, B. & SPARKS, R. S. J. 2005. Thermal constraints on the emplacement rate of a large intrusive complex: the Manaslu Leucogranite, Nepal Himalaya. *Journal of Petrology* **47**, 71–95.

BEAUMONT, C., JAMIESON, R. A., NGUYEN, M. H. & LEE, B. 2001. Himalayan tectonics explained by extrusion of a low-viscosity crustal channel coupled to focused surface denudation. *Nature* **414**, 738–42.

BEAUMONT, C., JAMIESON, R. A., NGUYEN, M. H. & MEDVEDEV, S. 2004. Crustal channel flows: 1. Numerical models with applications to the tectonics of the Himalayan-Tibetan orogen. *Journal of Geophysical Research* **109**, 1–29.

BERTHÉ, D., CHOUKROUNE, P. & JEGOUZO, P. 1979. Orthogneiss, mylonite and non-coaxial deformation of granites: the example from the south Armorican shear zone. *Journal of Structural Geology* **1**, 31–42.

CATLOS, E. J., HARRISON, T. M., KOHN, M. J., GROVE, M., RYERSON, F. J., MANNING, C. E. & UPRETI, B. N. 2001. Geochronologic and thermobarometric constraints on the evolution of the Main Central Thrust, central Nepal Himalaya. *Journal of Geophysical Research* **106**, 16177–204.

DASGUPTA, S., CHAKRABORTY, S. & NEOGI, S. 2009. Petrology of an inverted Barrovian sequence of metapelites in Sikkim Himalaya, India: constraints on the tectonics of inversion. *American Journal of Science* **309**, 43–84.

ENGLAND, P. C. & HOLLAND, T. J. B. 1979. Archimedes and the Tauern eclogites: the role of buoyancy in the preservation of exotic eclogite blocks. *Earth and Planetary Science Letters* **44**, 287–94.

EVANS, A. M. 1980. *An Introduction to Ore Geology*. Oxford: Blackwell Scientific Publications.

EXNER, U., GRASEMANN, B. & MANCKTELOW, N. S. 2006. Multiple faults in ductile simple shear: analogue models of flanking structure systems. In *Analogue and Numerical Modelling of Crustal-Scale Processes* (eds S. J. H. Butler & G. Shreurs), pp. 381–95. Geological Society of London, Special Publication no. 253.

FRASER, G., WORLEY, B. & SANDIFORD, M. 2000. High-precision geothermometry across the High Himalayan metamorphic sequence, Langtang Valley, Nepal. *Journal of Metamorphic Geology* **18**, 665–81.

GANGULI, J., DASGUPTA, S., CHENG, W. & NEOGI, S. 2000. Exhumation history of a section of the Sikkim Himalayas, India: records in the metamorphic mineral equilibria and compositional zoning of garnet. *Earth and Planetary Science Letters* **183**, 471–86.

GODIN, L., GRUJIC, D., LAW, R. D. & SEARLE, M. P. 2006. Channel flow, extrusion and extrusion in continental collision zones: an introduction. In *Channel Flow, Ductile Extrusion and Exhumation in Continental Collision Zones* (eds R. D. Law, M. P. Searle & L. Godin), pp 1–23. Geological Society of London, Special Publication no. 268.

GRASEMANN, B., EDWARDS, M. A. & WIESMAYR, G. 2006. Kinematic dilatancy effects on orogenic extrusion. In *Channel Flow, Ductile Extrusion and Exhumation in Continental Collisional Zones* (eds R. D. Law, M. P. Searle & L. Godin), pp 183–99. Geological Society of London, Special Publication no. 268.

GRUJIC, D., CASEY, M., DAVIDSON, C., HOLLISTER, L. S., KÜNDIG, R., PAVLIS, T. & SCHMID, S. 1996. Ductile extrusion of the Higher Himalayan Crystalline in Bhutan: evidence from quartz microfabrics. *Tectonophysics* **260**, 21–43.

GRUJIC, D., HOLLISTER, L. S. & PARRISH, R. R. 2002. Himalayan metamorphic sequence as an orogenic channel: insight from Bhutan. *Earth and Planetary Science Letters* **198**, 177–91.

HARRISON, T. M., RYERSON, F. J., LEFORT, P., YIN, A., LOVERA, O. M. & CATLOS, E. J. 1997. A Late Miocene–Pliocene origin for the Central Himalayan inverted metamorphism. *Earth Planetary Science Letters* **146**, E1–E8.

HOLLISTER, L. S. 1993. The role of melt in the uplift and exhumation of orogenic belts. *Chemical Geology* **108**, 31–48.

HOLLISTER, L. S. & GRUJIC, D. 2006. Pulsed channel flow in Bhutan. In *Channel Flow, Ductile Extrusion and Exhumation in Continental Collision Zones* (eds R. D. Law, M. P. Searle, L. Godin), pp. 415–23. Geological Society of London, Special Publication no. 268.

JAIN, A. K. & ANAND, A. 1988. Deformational and strain patterns of an intracontinental ductile shear zone – an example from the Higher Garhwal Himalaya. *Journal of Structural Geology* **10**, 717–34.

JAIN, A. K. & PATEL, R. C. 1999. Structure of the Higher Himalayan Crystallines along the Suru-Doda Valleys (Zanskar), NW Himalaya. In *Geodynamics of the NW Himalaya* (eds A. K. Jain & R. M. Manickavasagam), pp. 91–110. Gondwana Research Group Memoir no. 6.

KELLETT, D. A., GRUJIC, D., WARREN, C., COTTLE, J., JAMIESON, R. & TENZIN, T. 2010. Metamorphic history of a syn-convergent orogen parallel detachment: the South Tibetan detachment system, Bhutan Himalaya. *Journal of Metamorphic Geology* **28**, 785–808.

LEECH, M. L., SINGH, S., JAIN, A. K., KLEMPERER, S. & MANICKAVASAGAM, R. M. 2005. The onset of the India–Asia continental collision: early, steep subduction required by the timing of UHP metamorphism in the western Himalaya. *Earth and Planetary Science Letters* **234**, 83–97.

LI, Z. H., GERYA, T. V. & BURG, J. P. 2010. Influence of tectonic overpressure on P–T paths of HP–UHP rocks in continental collision zones: thermomechanical modeling. *Journal of Metamorphic Geology* **28**, 227–47.

LOMBARDO, B., PERTUSATI, P. & BORGHI, S. 1993. Geology and tectonomagmatic evolution of the eastern Himalaya along the Chomolungma-Makalu transect. In *Himalayan Tectonics* (eds P. Treloar & M. P. Searle), pp 341–55. Geological Society of London, Special Publication no. 74.

MANCKTELOW, N. S. 2006. How ductile are ductile shear zones? *Geology* **34**, 345–8.

MANCKTELOW, N. S. 2008. Tectonic pressure: theoretical concepts and modeled examples. *Lithos* **103**, 149–77.

MARCHILDON, N. & BROWN, M. 2003. Spatial distribution of melt-bearing structures in anatectic rocks from Southern Brittany, France: implications for melt transfer at grain- to orogen-scale. *Tectonophysics* **364**, 215–35.

MOORES, E. M. & TWISS, R. J. 1995. *Tectonics*. New York: W. H. Freeman and Company, 187 pp.

MUKHERJEE, S. 2011. Mineral fish: their morphological classification, usefulness as shear sense indicators and genesis. *International Journal of Earth Sciences* **100**, 1303–14.

MUKHERJEE, S. & KOYI, H. A. 2010*a*. Higher Himalayan Shear Zone, Sutlej section: structural geology and extrusion mechanism by various combinations of simple shear, pure shear and channel flow in shifting modes. *International Journal of Earth Sciences* **99**, 1267–303.

MUKHERJEE, S. & KOYI, H. A. 2010*b*. Higher Himalayan Shear Zone, Zanskar Indian Himalaya – microstructural studies & extrusion mechanism by a combination of simple shear & channel flow. *International Journal of Earth Sciences* **99**, 1083–110.

PAI, S.-I. 1956. *Viscous Flow Theory I – Laminar flow*. New Jersey: D. Van Nostrand, 51 pp.

PAPANASTASIOU, C. T., GEORGIOU, G. C. & ALEXANDROU, A. N. 2000. *Viscous Fluid Flow*. Florida: CRC Press.

PASSCHIER, C. W. & TROUW, R. A. J. 2005. *Microtectonics*. Heidelberg: Springer.

PATEL, R. C., SINGH, S., ASOKAN, A. & JAIN, A. K. 1993. Extensional tectonics in the Himalayan orogen, Zanskar, NW India. In *Himalayan Tectonics* (eds P. J. Treloar & M. P. Searle), pp. 445–59. Geological Society of London, Special Publication no. 74.

RAMSAY, J. G. 1980. Shear zone geometry: a review. *Journal of Structural Geology* **2**, 83–99.

RAMSAY, J. G. & LISLE, R. 2000. *The Techniques of Modern Structural Geology*, vol. **3**: *Applications of Continuum Mechanics in Structural Geology*. San Francisco: Academic Press, 926 pp.

REGENAUER-LIEB, K. & YUEN, D. A. 2003. Modeling shear zones in geological and planetary sciences: solid-and fluid-thermal-mechanical approaches. *Earth-Science Reviews* **63**, 295–349.

SCAILLET, B., HOLTZ, F. & PICHAVANT, M. 1996. Viscosity of Himalayan leucogranites: implications for mechanisms of granite magma ascent. *Journal of Geophysical Research* **101**, 27691–9.

SCHLICHTING, H. & GERSTEN, K. 1999. *Boundary Layer Theory*, 8th ed. Berlin: Springer.

SCHULMANN, K., LEXA, O., ŠTÍPSKÁ, P., RACEK, M., TAJČMANOVÁ, L., KONOPÁSEK, J., EDEL, J.-B., PESCHLER, A. & LEHMANN, J. 2008. Vertical extrusion and horizontal channel flow of orogenic lower crust: key exhumation mechanisms in large hot orogens? *Journal of Metamorphic Petrology* **26**, 273–97.

SELVERSTONE, J., MORTEANI, G. & STAUDE, J.-M. 1991. Fluid channelling during ductile shearing: transformation of granodiorite into aluminous schist in the Tauern Window, Eastern Alps. *Journal of Metamorphic Geology* **9**, 419–31.

STÜWE, K. 2007. *Geodynamics of the Lithosphere*, 2nd ed. Berlin: Springer, 325 pp.

TWISS, R. J. & MOORES, E. M. 2007. *Structural Geology*, 2nd ed. New York: W. H. Freeman and Company, 736 pp.

VALDIYA, K. S. 2001. Reactivation of terrane-defining boundary thrusts in central sectors of the Himalaya: implications. *Current Science* **81**, 1418–31.

VANNAY, J.-C. & GRASEMANN, B. 2001. Himalayan inverted metamorphism and syn-convergence extension as a consequence of a general shear extrusion. *Geological Magazine* **138**, 253–76.

VON HUENE, R., RANERO, C. R. & SCHOLL, D. W. 2009. Convergent margin structure in high-quality geophysical images and current kinematic and dynamic models. In *Subduction Zone Geodynamics* (eds S. Lallemand & F. Funiciello), pp. 137–57. Berlin, Heidelberg: Springer-Verlag.

WARREN, C. J., BEAUMONT, C. & JAMIESON, R. A. 2008*a*. Deep subduction and rapid exhumation: role of crustal strength and strain weakening in continental subduction and ultrahigh-pressure rock exhumation. *Tectonics* **27**, TC6002.

WARREN, C. J., BEAUMONT, C. & JAMIESON, R. 2008*b*. Formation and exhumation of ultra-high-pressure rocks during continental collision: role of detachment in the subduction channel. *Geochemistry Geophysics Geosystems* **9**, Q04019.

WARREN, C. J., BEAUMONT, C. & JAMIESON, R. A. 2008*c*. Modelling tectonic styles and ultra-high pressure (UHP) rock exhumation during the transition from oceanic subduction to continental collision. *Earth and Planetary Science Letters* **267**, 129–45.

WEBB, S. L. & DINGWELL, D. B. 1990. Non-Newtonian rheology of igneous melts at high stresses and strain rates: experimental results for rhyolites, andesites, basalt, and nephelinite. *Journal of Geophysical Research* **95**, 15695–701.

WEINBERGER, R., LYAKHOVSKY, V., BAER, G. & BEGIN, Z. B. 2006. Mechanical modeling and InSAR measurements of Mount Sedom uplift, Dead Sea basin: implications for effective viscosity of rock salt. *Geochemistry Geophysics Geosystems* **7**, Q05014.

WHIPPLE, K. 2009. The influence of climate on the tectonic evolution of mountain belts. *Nature Geoscience* **2**, 97–104.

WOBUS, C., HEIMSATH, A. & WHIPPLE, K. 2005. Active out-of-sequence thrust faulting in the central Nepalese Himalaya. *Nature* **434**, 1008–11.

YIN, A. 2006. Cenozoic tectonic evolution of the Himalayan orogen as constrained by along-strike variation of structural geometry, exhumation history, and foreland sedimentation. *Earth-Science Reviews* **76**, 1–131.

ZHAO, Z., NIU, Y., CHRISTENSEN, N. I., ZHOU, W., HOU, Q., ZHANG, Z. M., XIE, H., ZHANG, Z. C. & LIU, J. 2011. Delamination and ultra-deep subduction of continental crust: constraints from elastic wave velocity and density measurement in ultrahigh-pressure metamorphic rocks. *Journal of Metamorphic Geology* **29**, 781–801.

Appendix. Equations

The 'Poisson equation' of rectilinear flow of an incompressible Newtonian viscous fluid in the z-direction through a very long parallel rigid boundary inclined shear zone is given by eqn 6.190 of Papanastasiou, Georgiou & Alexandrou (2000):

$$(\partial^2 U_z/\partial x^2) + (\partial^2 U_z/\partial y^2) = \mu^{-1}\,[\partial P/\partial z - d\,g\,\mathrm{Sin}\theta] \quad (1)$$

https://doi.org/10.1017/S0016756811001075 Published online by Cambridge University Press

Here 'x' and 'y' are perpendicular directions and lie on the cross-section of the shear zone; U_z is the velocity of the fluid along the z-direction; 'μ' is the dynamic viscosity of the fluid; $(\partial P/\partial z)$ is the pressure gradient along the shear zone that forces the fluid to extrude; 'd' is the density of the fluid, 'g' is the acceleration due to gravity, and 'θ' is the dip of the shear zone.

If only the y–z cross-section of the flow is considered, then $(\partial^2 U_z/\partial x^2) = 0$. Thus,

$$(\partial^2 U_z/\partial y^2) = \mu^{-1}\,[\partial P/\partial z - d\,g\,\mathrm{Sin}\theta] \tag{2}$$

Integrating twice, taking the thickness of the shear zone to be $2y_0$ units, and considering the boundary conditions of simple shear on both the boundaries, i.e. at $y = y_0$, $U_z = U_1$, and at $y = -y_0$, $U_z = -U_2$ leads to the following flow profile:

$$U_z = 0.5\,\mu^{-1}\,[\partial P/\partial z - d\,g\,\mathrm{Sin}\theta]\,(y^2 - y_0^2) + 0.5\,\{y\,y_0^{-1}\,(U_1 + U_2) + (U_1 - U_2)\} \tag{3}$$

The vertex of the parabolic profile (3) is given by

$$z_1 = 0.5\,(U_1 - U_2) - 0.125\,\mu\,y_0^{-2}\,(U_1 + U_2)^2\,(\partial P/\partial z - d\,g\,\mathrm{Sin}\theta)^{-1} - 0.5\,\mu^{-1} y_0^2\,(\partial P/\partial z - d\,g\,\mathrm{Sin}\theta) \tag{4}$$

and, $$y_1 = -0.5\,y_0^{-1}\mu\,(U_1 + U_2)\,(\partial P/\partial z - d\,g\,\mathrm{Sin}\theta)^{-1} \tag{5}$$

For the absolute value of $\partial P/\partial z >$ than that of 'd g Sinθ', and U_1, $U_2 \neq 0$, both the 'z-' and the y-ordinates of the vertex are > 0 (Fig. 1b). For the absolute value of $\partial P/\partial z <$ than that of 'd g Sinθ', and U_1, $U_2 \neq 0$, both the 'z-' and the y-ordinates of the vertex are < 0 (Fig. 1c, d).

$\partial P/\partial z$ being < 0 (this is because, as 'z' increases, 'P' falls), 'y_1' is always > 0. Thus, using (5), the thickness of the sub-zone with a shear sense opposed to the remainder of the master zone is:

$$y_1' = y_0 - 0.5\,y_0^{-1}\,\mu\,(U_1 + U_2)\,(\partial P/\partial z - d\,g\,\mathrm{Sin}\theta)^{-1} \tag{6}$$

The thickness of the studied master shear zone is '$2y_0$' units. The remaining sub-zone where the shear sense is the same as that given by shearing of the boundaries is given by:

$$y_2' = y_0 + 0.5\,y_0^{-1}\,\mu\,(U_1 + U_2)\,(\partial P/\partial z - d\,g\,\mathrm{Sin}\theta)^{-1} \tag{7}$$

Clearly, $y_1' < y_2'$.

For $y_1 > y_0$ (profile 'B' in Fig. 2a, b), the vertex of the profile is outside the shear zone.

For $y_1 = y_0$ (profile 'A' in Fig. 2a, b), the vertex lies on the upper boundary of the shear zone.

To find the co-ordinate of the point of intersection between the *y*-axis and the velocity profile given by (3), $U_z = 0$ is inserted in (3):

$$0 = 0.5\,\mu^{-1}\,[\partial P/\partial z - d\,g\,\mathrm{Sin}\theta]\,(y^2 - y_0^2) + 0.5\,\{y\,y_0^{-1}\,(U_1 + U_2) + (U_1 - U_2)\} \tag{8}$$

Now if $U_2 = 0$ (Fig. 1e), (8) simplifies to:

$$0 = 0.5\,\mu^{-1}\,[\partial P/\partial z - d\,g\,\mathrm{Sin}\theta]\,(y^2 - y_0^2) + 0.5\,U_1\,(y\,y_0^{-1} + 1) \tag{9}$$

The point $(0, -y_0)$ is satisfied in (9). Thus $(0, -y_0)$ is the pivot.

Similarly, if $U_1 = 0$ (Fig. 1f), (8) simplifies to:

$$0 = 0.5\,\mu^{-1}\,[\partial P/\partial z - d\,g\,\mathrm{Sin}\theta]\,(y^2 - y_0^2) + 0.5\,U_2\{y\,y_0^{-1} - 1\} \tag{10}$$

The point $(0, y_0)$ is satisfactory with respect to (10). Thus $(0, y_0)$ is the pivot.

For $\partial P/\partial z = d\,g\,\mathrm{Sin}\theta$ (Fig. 1a), the co-ordinate of the pivot is derived from (8) as:

$$[0,\ y_0\,(U_2 - U_1)\,(U_2 + U_1)^{-1}] \tag{11}$$

When $\theta \neq 0$, and $U_1 = U_2 = \partial P/\partial z = 0$, the velocity profile in (3) simplifies to:

$$U_z' = -0.5\,\mu^{-1}\,[d\,g\,\mathrm{Sin}\theta]\,(y^2 - y_0^2) \tag{12}$$

And, for $\theta = 0$, and $U_1 = U_2 \neq 0$,

$$U_z'' = 0.5\,\mu^{-1}\,\partial P/\partial z\,(y^2 - y_0^2) + 0.5\,\{y\,y_0^{-1}\,(U_1 + U_2) + (U_1 - U_2)\} \tag{13}$$

When θ, U_1, U_2, $\partial P/\partial z \neq 0$,

$$U_z''' = 0.5\,\mu^{-1}\,[\partial P/\partial z - d\,g\,\mathrm{Sin}\theta]\,(y^2 - y_0^2) + 0.5\,\{y\,y_0^{-1}(U_1 + U_2) + (U_1 - U_2)\} \tag{14}$$

From (12)–(14):

$$U_z''' = (U_z' + U_z'') \tag{15}$$

https://doi.org/10.1017/S0016756811001075 Published online by Cambridge University Press